by total immersion into a constant-temperature oil bath. The tubes were removed after various amounts of time and cooled in cold water, and the extent of reaction was determined by ^1H NMR. Both the rate constants and activation parameters were determined with use of a linear least-squares fitting procedure. In order to monitor the cyclometalation of the two methylidene complexes **5a,b**, C_6D_6 solutions of the methylidene were first photogenerated in sealed 5-mm NMR tubes. The tubes were then placed in the temperature-controlled probe of a Varian XL200 spectrometer and kinetic data obtained by monitoring the decrease with time of the Ta–CH_2 resonance.

X-ray Diffraction Analysis. Crystal data and data collection parameters are collected in Table I. General operating procedures have been reported previously.[29]

$Ta(OAr')_2Me_3$ (2a). A suitable crystal, cleaved from a larger sample, was characterized by reciprocal lattice search techniques and found to be monoclinic, space group $C2$, Cm, or $C2/m$. Multan 78 was employed in each of the three possible space groups with only $C2$ yielding a solution. A Patterson synthesis as well as the subsequent refinement confirmed the space group. All atoms, including hydrogens, were located and refined. Although the molecular symmetry of the molecule is such that it could possess m symmetry, the final coordinates deviate from those needed for the higher point group. In the final full-matrix least-squares analysis the hydrogen atoms were assigned isotropic thermal parameters, all other atoms being refined anisotropically. A final difference Fourier was featureless with the exception of one peak of 1.24 e/Å^3 located at the tantalum site.

$Ta(OAr'\text{–}OMe)_2Me_3$ (2b). The sample consisted of perfectly formed yellow transparent crystals. A suitable crystal was transferred to the goniostat with use of standard inert atmosphere handling techniques and cooled to −159 °C. A systematic search of a limited hemisphere of reciprocal space located a set of diffraction maxima of orthorhombic symmetry with systematic extinctions corresponding to *Pnma* (or its noncentric equivalent). Solution and refinement of the structure were possible in the centric setting.

Due to air conditioning failure, the crystal was lost before data collection was complete, and 46 reflections in the $0k1$ zone were not recorded. It was decided that the lack of these data would not cause any systematic errors, so no attempt was made to recollect on a new crystal. All hydrogen atoms were located and refined isotropically with anisotropic thermal parameters for the non-hydrogen atoms.

A final difference Fourier was featureless, the largest peak being 0.72 e/Å^3. No absorption correction was made.

Acknowledgment. We thank the National Science Foundation (Grant CHE-8219206 to I.P.R.) for support of this research.

Supplementary Material Available: Tables of fractional coordinates of hydrogen atoms, anisotropic thermal parameters, complete bond distances and angles, and observed and calculated structure factors (39 pages). Ordering information is given on any current masthead page.

(29) Huffman, J. C.; Lewis, L. N.; Caulton, K. G. *Inorg. Chem.* **1980**, *19*, 2755.

An Unusual Trimetallic Cluster and Its Hypothetical Solid-State Counterparts

Marjanne C. Zonnevylle, Jérôme Silvestre, and Roald Hoffmann*

Contribution from the Department of Chemistry and Materials Sciences Center, Cornell University, Ithaca, New York 14853. *Received September 16, 1985*

Abstract: The electronic structure of the $Cp_2Co_3(CO)_4^{2-}$ core of the recently synthesized $Cp_3Co_3(CO)_4(YbCp_2)_2$ molecule is analyzed by a fragment orbital molecular orbital analysis. The odd electron in this unusual linear trinuclear complex should occupy a metal and Cp based orbital of special symmetry. Reduction may lead to Co–Co bond lengthening and a tetrahedral geometry at the central Co. The relationship to $Fe_3(CO)_{11}^{2-}$ and allene is traced. The series $CpCo(CO)_2$, $Cp_2Co_2(CO)_2$, and $Cp_2Co_3(CO)_4^{2-}$ leads us to think of several alternative and as yet unsynthesized $Co(CO)_2$ polymers.

Among the multitude of trimetalic clusters known today, few of those built upon a metal–metal bonded framework abandon the triangular geometry typified by the series $M_3(CO)_{12}$, M = Fe, Ru, Os[1a–c] (**1**). An early known example of such a dissenter is Dahl's $Fe_3S_2(CO)_9$ (**2**), which features only two Fe–Fe bonds.[2] The backbone angle α, that is, the angle between the two metal–metal bonds, is only 81.0°. The complex is still best described as triangular, albeit open triangular. Its desire to keep one bond

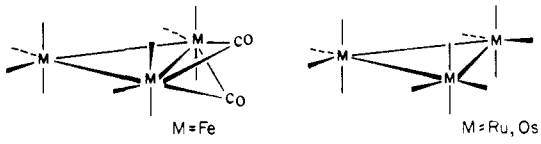

1

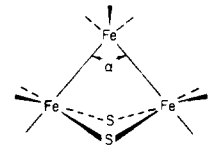

2

long is easily understood within the framework of skeletal electron pair counting schemes such as those of Wade and Mingos.

Moving toward a more linear geometry, we find $Fe_3(CO)_{11}[Cp^*_2Yb]_2$ (where $Cp^* = C_5Me_5$) which also has two Fe–Fe bonds, but the backbone angle is now opened[3] to ~162°, as depicted in **3**. We shall return to this complex shortly. For now, suffice it to notice that the $Fe_3(CO)_{11}^{2-}$ core, **3**, carries four bridging and seven terminal carbonyl groups. Of the latter, six are symmetrically distributed on the two end-iron atoms. The seventh one is located on top of the central Fe atom, at the apex

(1) (a) Cotton, F. A.; Troup, J. M. *J. Am. Chem. Soc.* **1974**, *96*, 4155. (b) Mason, R.; Rae, A. I. B. *J. Chem. Soc. A.* **1968**, 778. (c) Corey, E. R.; Dahl, L. F. *Inorg. Chem.* **1962**, *1*, 521.

(2) Wei, C. H.; Dahl, L. F. *Inorg. Chem.* **1965**, *4*, 493. See also Bard, A. J.; Cowley, A. H.; Leland, J. K.; Thomas, J. N.; Norman, N. C.; Jutzi, P.; Morley, C. P.; Schlüter, E. *J. Chem. Soc., Dalton Trans.* **1985**, 1303.

(3) Tilley, T. D.; Andersen, R. A. *J. Am. Chem. Soc.* **1982**, *104*, 1772.

0002-7863/86/1508-1509$01.50/0

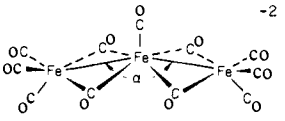

3

of a square pyramid. The four bridging CO's lie in approximately coplanar pairs across the Fe–Fe bonds. These pairs in the complete molecule are clamped by two $[YbCp^*_2]^+$ units, as shown in **4** from a top view.

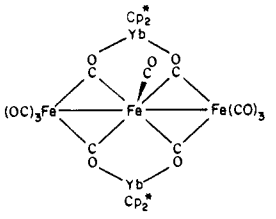

4

Intimately related to **4** is another complex recently reported by Andersen,[4] $Co_3Cp_2(CO)_4[YbCp^*_2]_2$, Cp = $C_5H_4SiMe_3$. Again, omitting the $[YbCp^*_2]^+$ fragments, the framework may be pictured schematically as in **5**. The structure is essentially planar, save the Cp rings which lie perpendicular to the molecular plane. The backbone angle α in **5** is 176.5°. There are two other peculiar

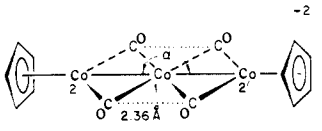

5

structural features contained within **5**: namely, two short Co–Co distances of 2.36 Å and two relatively close contacts between the carbon atoms of the bridging CO ligands, also ~2.36 Å.

In both **3** and **5** we have stripped away the $[YbCp^*_2]^+$ fragments. The reason for this is that we would like to consider these units as simple Lewis acids. The electronic structure of $LnCp_2^+$ fragments is discussed elsewhere;[5] these important d^0f^x units contain several low-lying acceptor orbitals suitable for interactions with the oxygen lone pairs of the carbonyls in what are then formally $Fe_3(CO)_{11}^{2-}$ and $Co_3Cp_2(CO)_4^{2-}$ anions.

Returning to **5**, the structure features a highly unusual sixfold planar coordination around the central cobalt atom, Co_1. Other examples of this environment are not surprisingly scarce in organometallic chemistry. Perhaps we should mention here the cluster anions $Pt_2Rh_{11}(CO)_{24}^{3-}$ and $PtRh_{12}(CO)_{24}^{4-}$ and the isoelectronic series $[Rh_{13}H_{5-n}(CO)_{24}]^{n-}$, n = 2, 3, 4.[6] The metal atoms of these isomorphic clusters form hexagonal close-packed cages such that one metal atom lies at the center of a hexagon capped above and below by triangular metallic units. Six-coordination is also a common feature of uranyl chemistry.

Complex **5** is a 47-electron cluster. More specifically we have 27 d electrons to distribute over three metallic centers. The motivation for this work may be summarized in the following basic questions. Where does the odd electron reside? How can we describe the metal–metal bonding in **5**? What could be the structural consequence of oxidation or reduction of the system? Is the planarity of **5** forced by the $YbCp^*_2$ units or is this geometry inherently more stable than other alternatives? Can the short C–C distance translate into bonding?

Aside from these questions, the structure of **5** is of interest to us in our quest to perceive the continuity that must exist between the realms of discrete and extended structures. It is indeed tempting to visualize **5** as the trimer of a series of oligomers of which the monomer and dimer representatives are $CoCp(CO)_2$[7a–c] (**6**) and $Co_2Cp_2(CO)_2^n$ (n = 0, −1)[8a–c] (**7**), respectively. Many complexes related to the monomer **6** have been reported in the

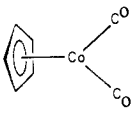

6

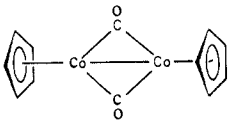

7

literature.[9] Similarly, the dimeric structure **7** belongs to a voluminous set of extensively studied[10] isomorphic structures. These are derived by successive replacement of the carbonyls by nitrosyls[11] and/or exchange of one or both of the cobalt atoms for nickel,[12a] iron,[12b] rhodium,[13] or iridium.[14] In light of the flexibility exhibited within this series of complexes, it is not surprising that recently synthesized rhodium and iridium compounds of formula $M_3Cp_2(CO)_9$ $[YbCp^*_2]_2$ appear to be isostructural to **5**.[15]

Is this kind of system and the chemistry thereof sufficiently flexible to accommodate a polymeric structure? If so, it has yet to be discovered. Let us envisage just a handful of the numerous structural possibilities. For instance, a simple extension of **5** gives the flat ribbon **8**. A twist of the coordination about Co_1 (see **5**)

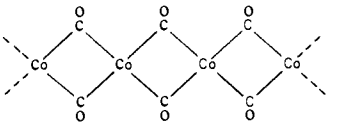

8

to produce the hypothetical tetrahedral (at Co_1) trimer **9** may suggest a polymeric analogue such as **10**. Puckering the carbonyls of **5**, we can hypothesize two versions of a kinked ribbon, **11a** and

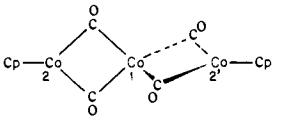

9

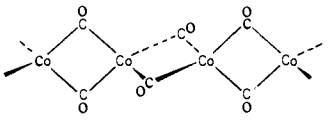

10

11b. Combining two ribbons of type **11a** leads to **12**. Even a two-dimensional framework can be constructed as in **13**. All these polymeric structures satisfy the $Co(CO)_2$ stoichiometry. Several

(4) Boncella, J. M.; Andersen, R. A. *J. Chem. Soc., Chem. Comm.* **1984**, 809.
(5) Ortiz, J. V.; Hoffmann, R. *Inorg. Chem.* **1985**, *24*, 2095.
(6) Fumagalli, A.; Martinengo, S.; Ciani, G. *J. Chem. Soc., Chem. Comm.* **1983**, 1381.
(7) (a) Byers, L. R.; Dahl, L. F. *Inorg. Chem.* **1980**, *19*, 277. (b) Piper, T. S.; Cotton, F. A.; Wilkinson, G. *J. Inorg. Nucl. Chem.* **1955**, *1*, 165. (c) Fisher, E. O.; Jira, R. *Z. Naturforsch. B.* **1955**, *10*, 355.
(8) (a) Bailey, W. I.; Collins, D. M.; Cotton, F. A.; Baldwin, J. C.; Kaska, W. C. *J. Organomet. Chem.* **1979**, *165*, 373. (b) Ginsburg, R. E.; Cirjak, L. M.; Dahl, L. F. *J. Chem. Soc., Chem. Comm.* **1979**, 468. (c) Schore, N. E.; Hender, C. S.; Bergman, R. G. *J. Am. Chem. Soc.* **1979**, *98*, 255, 256.
(9) (a) Fisher, E. O.; Brenner, K. S. *Z. Naturforsch. B.* **1962**, *17*, 774. (b) Fisher, E. O.; Bittler, K. *Z. Naturforsch. B.* **1961**, *16*, 225. (c) Macomber, D. W.; Spink, W. C.; Rausch, M. D. *J. Organomet. Chem.* **1983**, *250*, 311. (d) Hart, W. P.; Shihua, D.; Rausch, M. D. *J. Organomet. Chem.* **1985**, *282*, 111.
(10) (a) Pinhas, A. R.; Hoffmann, R. *Inorg. Chem.* **1979**, *18*, 654. (b) Dudeney, N.; Green, J. C.; Kirchner, O. N.; Smallwood, F. S. J. *J. Chem. Soc., Dalton Trans.* **1984**, 1883. (c) Bénard, M. *J. Am. Chem. Soc.* **1978**, *100*, 7740.
(11) Bernal, I.; Korp, J. D.; Reisner, G. M.; Herrmann, W. A. *J. Organomet. Chem.* **1977**, *139*, 321.
(12) (a) Byers, L. R.; Dahl, L. F. *Inorg. Chem.* **1980**, *19*, 680. (b) Calderon, J. L.; Fontana, S.; Frauendorfer, E.; Day, V. W.; Iske, D. A. *J. Organomet. Chem.* **1974**, *64*, C16.
(13) (a) Nutton, A.; Maitlis, P. M. *J. Organomet. Chem.* **1979**, *166*, C21. (b) Green, M.; Hankey, D. R.; Howard, J. A. K.; Louca, P.; Stone, F. G. A. *J. Chem. Soc., Chem. Comm.* **1983**, 757.
(14) Herrmann, W. A.; Barnes, C. E.; Serrano, R.; Kombouris, B. *J. Organomet. Chem.* **1983**, *256*, C30.
(15) Private communications from R. Andersen, April 15, 1985.

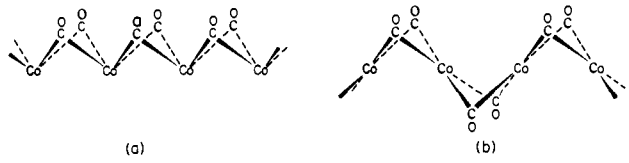

11

of the structures **8–13** will be analyzed later in the text.

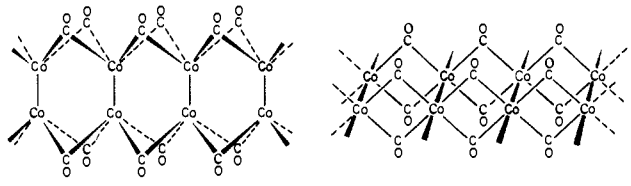

12 13

To begin, some electron counting is in order to describe the electronic structure of **5**. It is enlightening to first consider that of the *singly* charged species, $Co_3Cp_2(CO)_4^-$. At this point we ignore metal–metal bonding; counting each Cp as an anionic six-electron donor and the bridging CO's as neutral one-electron donors to each metal, we arrive at an overall 1– charge by assigning a 1– oxidation state to the central cobalt (Co_1) and 1+ oxidation state to the end ones (Co_2, Co'_2). As shown at the top of scheme **14**, Co_1 is in a d^{10} electronic configuration and surrounded by 14 electrons whereas $Co_2(Co'_2)$ is d^8 with 16 electrons around it. Following the scheme downwards, the creation of 2 metal–metal bonds gives $16e^-$ and $17e^-$ at the central and terminal cobalt atoms, respectively. If each Co–Co bond is assigned to be of order 2, an $18e^-$ count is reached at each metal center. Now add one electron to match the true electron count of **5**; this will formally

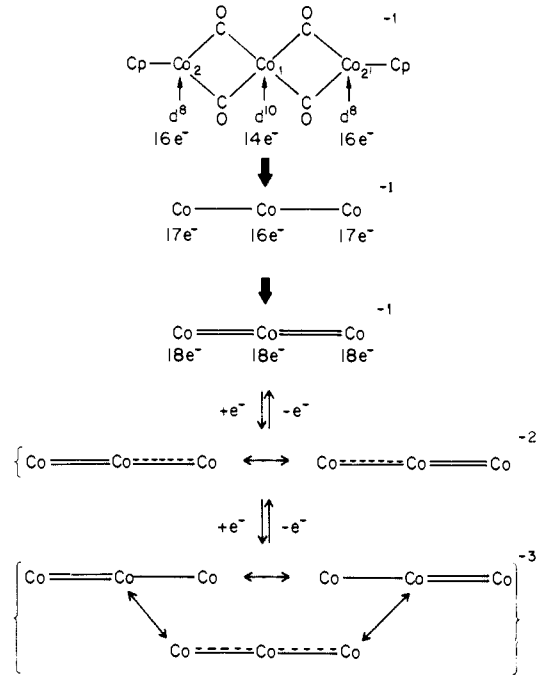

14

break one-half of a π bond. Reducing **5** by 1 electron will completely eliminate one π bond, thereby delocalizing two π electrons over three metal centers. From these qualitative considerations the idea of "electrochemical breathing" emerges, one electron oxidation (reduction) of **5** should contract (elongate) the metal–metal distances. The forthcoming MO analysis will confirm this point and as a byproduct will give some information as to the whereabouts of the odd electron.

The calculations are of extended Hückel type, with computational and geometrical details gathered in the Appendix.

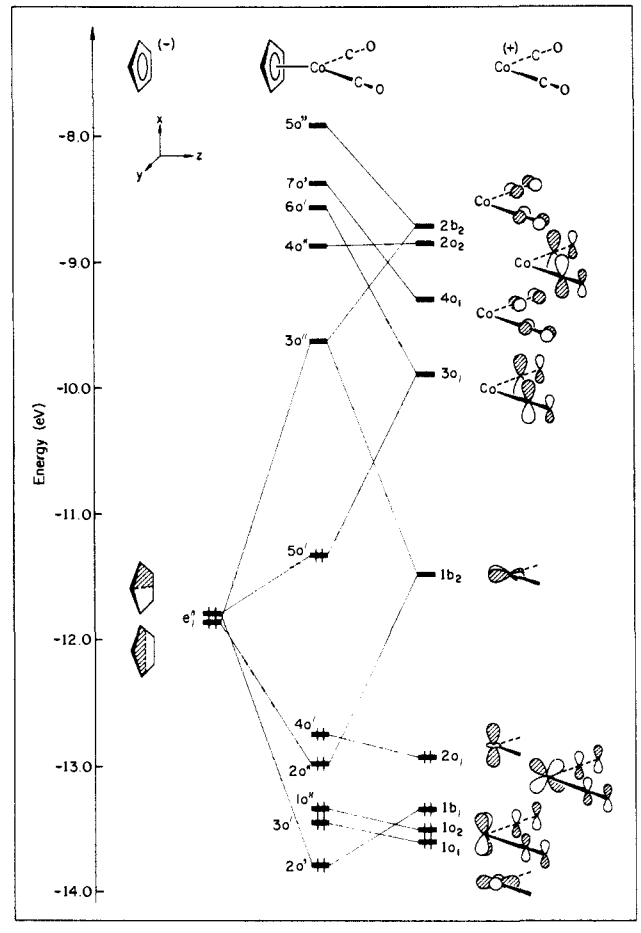

Figure 1. Interaction diagram for Cp and C_{2v}-$Co(CO)_2$ fragments of the $CpCo(CO)_2$ monomer.

A four-step process, outlined in **15**, may be used to construct systematically the molecular orbitals diagram of the planar system **5**. First the monomer $CpCo(CO)_2$ is assembled. Then, the carbonyls are bent back toward the Cp ring and two such units

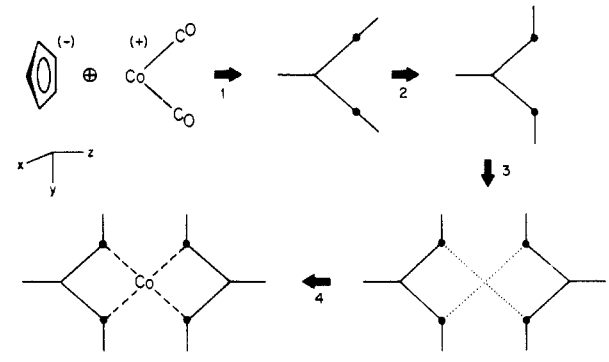

15

are brought together at the correct spacing for the incipient trimer. The central cobalt is finally inserted to complete the system.

Figure 1 constructs the MO pattern for the "monomer" $CpCo(CO)_2$. On the left is the bonding e''_1 set of a Cp ring. The third filled π orbital is at low energy and is not shown. The right-hand side of the figure shows the fragment MOs of the C_{2v}-$Co(CO)_2$ unit. These orbitals have been derived elsewhere[16] and we find the expected 4-below-1 pattern for the d-block. Higher in energy we have drawn out the carbonyl centered orbitals, since

(16) See for instance: (a) Burdett, J. K. *J. Chem. Soc., Faraday Trans.* **1974**, *2*, 1599. (b) Albright, T. A.; Burdett, J. K.; Whangbo, M.-H. "Orbital Interactions in Chemistry"; John Wiley & Sons: New York, 1985. (c) Albright, T. A. *Tetrahedron* **1982**, *38*, 1339.

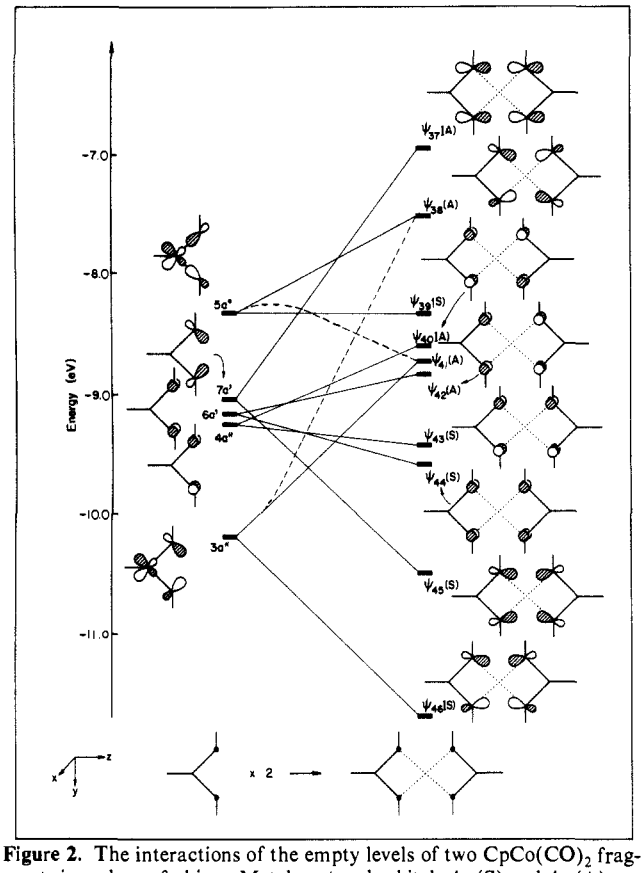

Figure 2. The interactions of the empty levels of two $CpCo(CO)_2$ fragments in a planar fashion. Metal-centered orbitals $\psi_{39}(S)$ and $\psi_{41}(A)$ are not drawn.

they are the ones that will play a crucial role in anchoring the unique cobalt atom in the trimer.

The interaction between the two fragments generates the pattern displayed in the middle of the figure. The lowest four d orbitals remain relatively unaltered by the perturbation. The x^2, xy, and $y^2 - z^2$ levels are slightly pushed up by the lower lying Cp orbitals. More important is the stabilization of xz. It emerges as the lowest state out of a 3-level interaction pattern; xz combines with both a component of Cp e''_1 and a carbonyl π^*. The middle nonbonding orbital thus produced is primarly Cp centered with a 27% admixture of cobalt xz; this is the HOMO of the complex. Another three-MO interaction is turned on and involves the other Cp e''_1 component, a carbonyl π^*, and yz of the metal. The metal orbital ($3a''$) emerges as the LUMO of $CpCo(CO)_2$. Incidentally we have formed the normal pattern corresponding to a d^8 - 18 electron organometallic complex.[17] However, the crucial point is that this molecule will be further coordinated, and this will involve the empty carbonyl centered orbitals. Because of their relative localization, these MOs are predestined to play a primary role in the ultimate binding mode of the trimer.

We will not dwell on the second step of **15** in which the CO's are bent back, in anticipation of further bonding. Not much happens in the medal-d and Cp centered MOs. We merely comment that due to an avoided crossing, molecular orbital $3a''$ (the LUMO) and the highest CO π^* exchange their character.

Figure 2 traces the third step, i.e., the juxtaposition of two such "bent monomers" so that the C–C spacing along the z axis is 2.36 Å as in the trimer. The figure delineates what happens to the empty levels, those centered on the CO groups. Clearly the metal–d and Cp centered levels split very little since the Co···Co distance is 2.36 × 2 = 4.72 Å. But these CO-centered levels, the ones shown in Figure 2, interact strongly. Each level on the left gives rise to two molecular orbitals: a symmetric (S) and an antisymmetric (A) partner. The S and A labels refer to the xy plane running between the two units. The two in-plane carbonyl π^* levels become four: $\psi_{46}(S)$, $\psi_{45}(S)$, $\psi_{38}(A)$, and $\psi_{37}(A)$. The splitting is large since the carbon lobes of one unit point directly toward the lobes of the other, generating a σ type of overlap. An avoided crossing between one of the π^* levels and one of the combinations descending from yz on metal complicates matters only slightly and is indicated with dashed lines in the figure.

Now we can begin to appreciate the effect of the aforementioned close C···C contact along the z axis: compare the 4.2-eV spread between the highest and lowest energy carbonyl π^* level of $[CpCo(CO)_2]_2$ on the right to the 1.0-eV range for the "bent monomer" on the left. The potential for a substantial interaction between the formally nonbonded carbons in the trimer is clear. A partial occupation of $\psi_{46}(S)$ and/or $\psi_{45}(S)$ mediated by the central cobalt atom will induce some C···C bonding. Of the ten molecular orbitals "awaiting" the central cobalt shown on the right of Figure 2, four are of σ type, four of π type, and two descend from yz of Figure 1 and are metal-d centered ($\psi_{39}(S)$ and $\psi_{41}(A)$). As expected the latter two split to a minimal extent due to the localization of the fragment lobes away from the coupling direction.

The final step of the procedure outlined in **15** is the insertion of the central cobalt atom into the sixfold vacancy defined by the 4 carbonyl groups and the 2 cobalt atoms. Since there is such a preponderance of levels, we have, for the sake of clarity, partitioned the overall MO scheme into two different panels. Disregarding the small asymmetry introduced by the Cp rings, one can classify the interactions into two types: those involving orbitals symmetric (σ) with respect to the yz plane (the plane containing the three cobalts and four carbonyls) and those featuring MOs antisymmetric (π) with respect to this plane. Thus Figure 3 displays a double interaction diagram: the left-hand side shows how the σ type of orbitals of the two fragments combine whereas the right-hand side of the figure describes the π-type interactions. Note that here the labels σ and π are not rigorous symmetry descriptors but classify pseudosymmetry and are used as simple pointers for our discussion. The complete molecular orbital pattern for **5** is a superposition of the two partial interaction diagrams.

The levels of $[CpCo(CO)_2]_2$ are divided between the central two columns as described above. The highest levels, $\psi_{46}(S)$ through $\psi_{37}(A)$, are those previously pictured at the right in Figure 2. As mentioned earlier, the lowest levels can be derived virtually without any computation from Figure 1. We know that the corresponding MOs of the monomer are either Cp or metal d centered. The distance, and hence the overlap, factor prevents any large interactions from taking place. Thus, MOs $\psi_{47}(A)$ down to $\psi_{58}(S)$ result from a simple doubling of the pattern displayed in Figure 1 below −11.0 eV. Moreover, the orbital compositions are essentially carried over directly from those in the monomer. For example, the character of $e''_1(S)$ in Figure 1 is mirrored in that of $\psi_{47}(A)$ which consists of 54% Cp and 29% cobalt. Below $\psi_{47}(A)$ and its symmetric mate $\psi_{48}(S)$ lie ten tightly packed levels. Two of them, $\psi_{49}(A)$ and $\psi_{51}(S)$, originate from the Cp-centered e''_1 monomer level and the remainder from the 4 low-lying metal-d orbitals.

Two d orbitals of the central cobalt, xz and yz, are of the proper symmetry to interact with out-of-plane $[CpCo(CO)_2]_2$ fragment orbitals. They are found at the far right of Figure 3. Cobalt x belongs to this column as well but is omitted from the diagram.

The out-of-plane (π) trimer MOs lie between the two out-of-plane fragment MO columns, completing the first half of the full interaction diagram. As indicated in the figure, it is in this column that we find the HOMO (circled) of our trimer **5**. More specifically this singly occupied orbital is the highest level produced by the 3-fold interaction between $\psi_{47}(A)$, $\psi_{57}(A)$, and xz. Therefore, it is primarily centered on the two terminal cobalt atoms and the Cp rings but carried a substantial contribution from the central metal atom, 15%. This orbital is explicitly drawn out in **16**, which emphasizes the antibonding relationship existing between adjacent cobalt atoms. The occupation of π_{50} partially destroys the π bonding provided by lower lying π_{67} depicted in **17**, and to a smaller extent π_{63}, **18**. Clearly, the contribution of x in the

(17) Hofmann, P. *Angew. Chem.* **1977**, *89*, 551; *Int. Ed. Engl.* **1977**, *16*, 536.

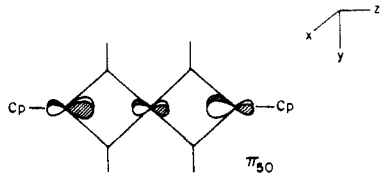

16

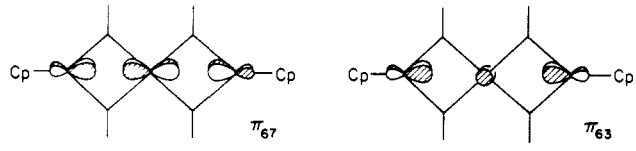

17 18

latter is smaller due to the large energy difference existing between x and ψ_{58}(S).

The reader may already anticipate how the occupation number of π_{50} will alter the geometry of the system, but we defer a more complete discussion of that topic to a later section of the text.

For now, let us focus on the left-hand side of Figure 3, that is on the interactions of σ type. The left-hand-most column of the figure presents the three in-plane cobalt d orbitals. Again for reasons of clarity, we omit the s,[18] y, and z atomic levels of the cobalt. There are two types of interaction which anchor the central cobalt atom into the framework, namely the metal–metal and central cobalt–carbonyl ones, and one, the carbon–carbon type, which stabilizes the framework itself.

Most of the metal–metal interaction comes from central cobalt yz combining with both ψ_{49}(A) and high-lying ψ_{41}(A). The lowest two levels thus produced are filled (σ_{60}, σ_{53}) whereas the top antibonding one is empty. Molecular orbital σ_{60} is sketched in **19**.

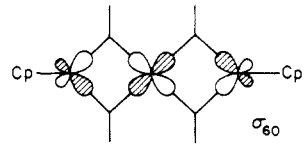

19

In spite of the substantial difference in energy, a significantly large overlap population of 0.28 is found between ψ_{41}(A) and yz. Another source of metal–metal bonding lies in the interaction between the high-lying z and the pair ψ_{50}(A), ψ_{53}(A). The bonding combination arising from the 3-fold mixing is sketched in **20**.

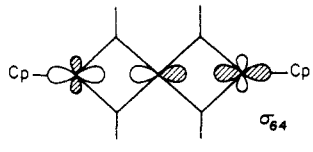

20

There are additional contribution to metal–metal bonding coming via through-bond coupling of the carbonyl-centered orbitals with those of the central cobalt atom. This brings us to the analysis of the central cobalt–carbonyl bonding. We find two main contributions, depicted in **21a–b**, involving z^2 and yz, respectively. The former matches ψ_{45}(S) in symmetry and the latter ψ_{41}, forming respectively the two bonding orbitals σ_{66} and σ_{53}.

Note that σ_{66} provides some C–C bonding. In fact, fragment orbital ψ_{45}(S), which is initially empty and carbon–carbon bonding, ends up with 0.43 e. The other important source of electron density between the carbon atoms of adjacent CO groups results from

(18) The cobalt s orbital lies at −9.21 eV. Because of the relatively low symmetry of the system it tends to mix with all symmetric orbitals. Its removal from the diagram of Figure 3 does not alter the conclusions of the present discussion.

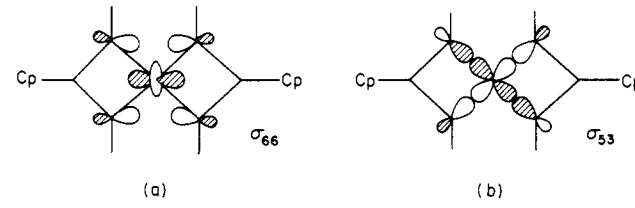

21

the populations of ψ_{46}(S). This orbital is so strongly depressed in energy by central Co y that the resulting MO, **22**, is filled by 2 electrons. The occupation of ψ_{46}(S) is 1.78 e.

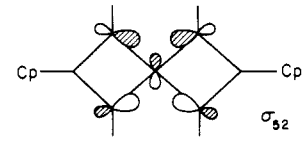

22

There is definitely C···C bonding in the trimer. Were ψ_{45}(S) and ψ_{46}(S) both completely filled, the dotted lines in **23** could be drawn as full σ bonds. We are not quite there but not that far

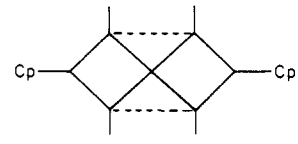

23

away either; *there is some carbon–carbon bonding in the trimer* **5**. A positive overlap population of 0.096 is computed between each pair of carbon atoms linked by the dotted lines in **23**.

From the patterns obtained in Figure 3, we can assign a formal oxidation state to each metal atom. Out of the ten d orbitals belonging to the terminal cobalt atoms, only the two descending from ψ_{41}(A) and ψ_{39}(S) emerge empty. Thus each end cobalt is approximately d^8. The five d orbitals of the central cobalt are filled. In essence, all of them are engaged in four-electron two-orbital interactions. It is only via mixing of high-lying empty Co-centered levels that some metal–metal bonding can exist. Therefore the central atom may be thought of as d^{10}. The additional electron is housed in π_{50} which *formally* descends from a Cp centered orbital. We saw earlier that metal d character is also present (overall 46%). For a monoanionic version of our trimer the electron configuration favored according to Figure 3 is d^8–d^{10}–d^8, in agreement with the qualitative treatment of scheme **14**.

From the picture developed so far, we would like to return temporarily to the complex shown in **4**. Stripping away the two $YbCp^*_2$ units and the apical CO ligand leaves a $[(CO)_3Fe(CO)_2]_2Fe^{2-}$ framework isoelectronic to **5** minus 1 electron. Its electronic structure should be similar to that obtained in Figure 3, the only difference being the absence of the odd electron in π_{50}. Why would a CO group bind to a one-electron oxidized analogue of **5**? The CO lone pair *cannot* be stabilized by π_{50} for symmetry reasons. Worse than that, the lone pair enters a destabilizing interaction with π_{51} which does contain a little z character on the central cobalt (~3%). However, orbital π_{50} is ideally set up to interact with one of the CO π^* orbitals. The carbonyl adduct is expected to be stable if the bonding combination between π_{50} and CO π^*, **24**, falls *below* the antibonding MO between the lone pair and π_{49}, **25**. A single calculation on $[CpCo(CO)_2]_2Co(CO)^-$ shows that this is indeed the case, **24** being the HOMO of the

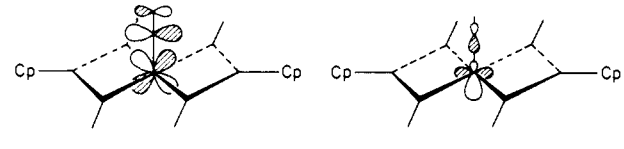

24 25

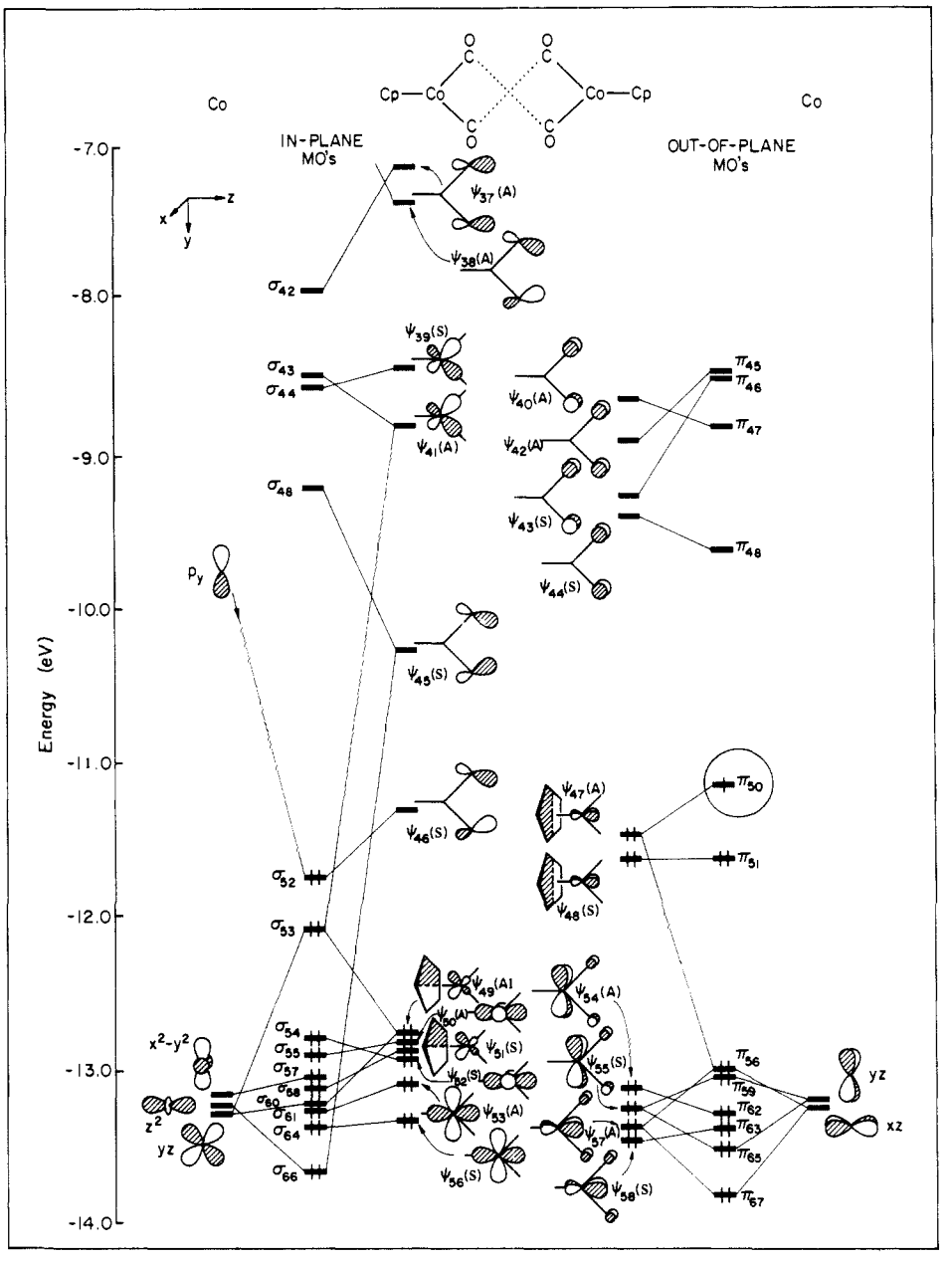

Figure 3. The interaction of the central cobalt and $[CpCo(CO)_2]$ fragments of $Co_3Cp_2(CO)_4^{2-}$. The fragment and molecular orbitals are segregated into two partial interaction diagrams, in-plane (σ) on the left and out-of-plane (π) on the right; see text.

Table I. Some Comparative Results for Planar and Perpendicular Geometries of $Cp_2Co_3(CO)_4^{q}$[a]

structure	charge q	Co–Co	C–C	O–O	ΔE, kcal/mol
planar, **26**	−1	0.098	0.096	−0.004	5.5
	−2	0.081	0.096	−0.004	[0]
	−3	0.065	0.095	−0.004	[0]
rotated, **27**	−1	0.112	0.010	0.000	[0]
	−2	0.090	0.012	0.000	8.5
	−3	0.068	0.013	0.000	22.6

[a] The Co–Co, C–C, and O–O columns tabulate overlap populations. For each electron count, the zero in energy is the total energy of the more stable geometry.

complex. In **25**, the $x^2 - z^2$ character of central cobalt derives from additional mixing with π_{51}. A calculation was also performed[19] to bring the CO down to the central cobalt atom; a large positive overlap population develops between Co and the carbon atom.

There is a relationship between the axial carbonyl addition to this Fe_3 complex and the 20-electron macrocyclic–Cu–carbonyl complexes of Gagne and co-workers.[20a] Their electronic structure has been analyzed by Burdett and Williams.[20b]

In this section we tackle the question of the stability of the planar framework **26**, such as the one adopted by **5**, relative to that of the rotated geometry such as **27**. In particular, we focus on the influence of the total number of electrons upon the geometry.

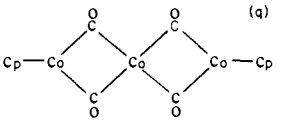

26

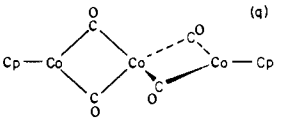

27

(19) This calculation by no means is intended to model the formation of **4**. In fact, one realizes easily that the addition of one CO on top of the central metal atom is a symmetry forbidden process. Experimentally, **4** is generated from $Fe_3(CO)_{12}$ which apparently provides the $Fe(CO)_5$ unit.

(20) (a) Gagné, R. R. *J. Am. Chem. Soc.* **1976**, *98*, 6709; Gagné, R. R.; Allison, J. L.; Lisensky, G. *Inorg. Chem.* **1978**, *17*, 3563. (b) Burdett, J. K.; Williams, P. D. *Ibid* **1980**, *19*, 2779.

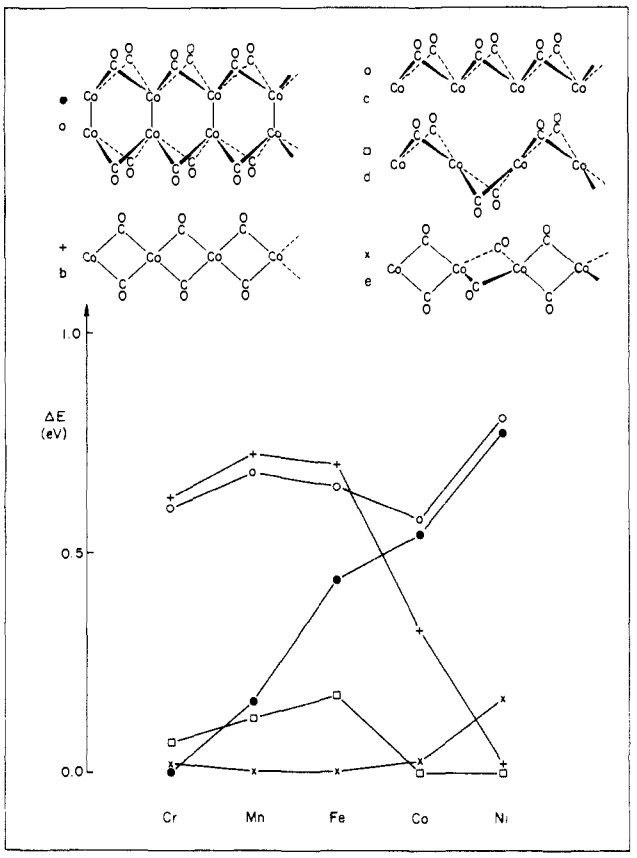

Figure 4. Relative energies (zero is the most stable structure) of several hypothetical polymeric $Co(CO)_2$ chains.

The pertinent results are collected in Table I. For each electron count the zero in energy was chosen to be that of the total energy of the more stable molecule. A glance at the Co-Co overlap population confirms our earlier suggestion of "electrochemical breathing". Starting from the isolated dianionic species, the removal or addition of one electron does indeed lengthen or shorten respectively the Co–Co bonds. The clue to understanding this result lies in the antibonding topology of the HOMO π_{50}. However, the calculations on **27**, the rotated isomer, indicate that the latter should be more stable for an oxidized complex. Since the energy difference is small, any argument is tenuous at this level of computation. The counterions (Cp_2Yb^+ for instance) could play a role in determining the preferred structure. There is, however, evidence of stronger Co–Co bonding in **27** than in **26**. This is understandable in view of **14** which shows that the monoanionic complex should exhibit two formal metal–metal double bonds. The D_{2d} geometry of **27** allows by symmetry a better localization of the π electrons in MO's such as **28a,b**. The electron density is exclusively shared by two metal atoms in each of the

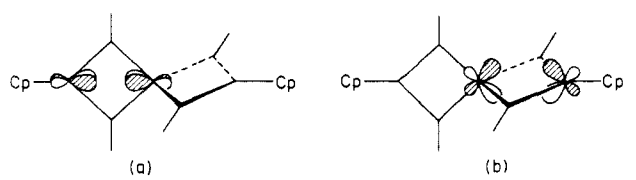

28

two degenerate levels **28a,b**. In contrast, the strength of the two π bonds in the coplanar isomer **26** is hampered by delocalization over three centers.[21]

We are now very close to an analogy between $Cp_2Co_3(CO)_4^-$ and allene, and for good reasons. If we were to "unbridge" the four carbonyls in $Cp_2Co_3(CO)_4^-$, a process that might not be very costly in energy, we would reach **29**, $[CpCo(CO)][Co(CO)_2^-][CpCo(CO)]$. $CpCo(CO)$ is isolobal[22] with $Fe(CO)_4$ and CH_2. $Co(CO)_2^-$, a d^{10} ML_2 fragment, is isolobal with CH_2^{2+}, which in turn is isolobal with a neutral carbon atom. The chain runs as follows:

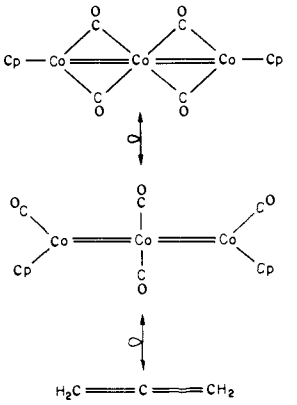

29

This is not just a formalism; the orbitals **28a,b** are, of course, the analogues of the localized π bonding orbitals of allene. Why then does further reduction cause a change in preferred geometry? It does so in allene, whose anions prefer planarity,[23] and in our $Cp_2Co_3(CO)_4^{2,3-}$. In allene the next orbitals to be filled are shown in **30** at the top and in the cobalt trimer in **30** at the bottom. Clearly a less antibonding orbital is filled in the planar geometry.

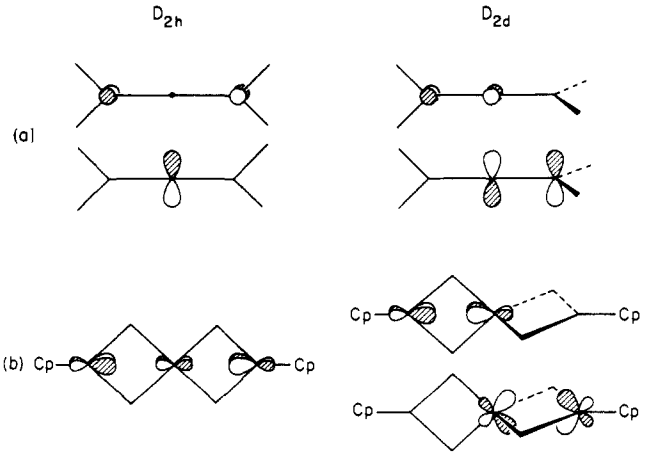

30

To close this section we should mention that another geometrical isomer of the trimer was examined numerically, namely that featuring a puckered frame as in **31**. This alternative had the merit of allowing geometrically for the binding of each $YbCp_2^*$ unit

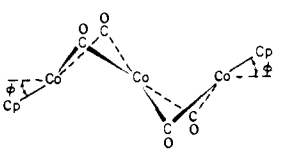

31

to two oxygen atoms. The oxygen pair would be those sitting across the metal–metal frame, rather than alongside, as in the observed system. A number of exploratory calculations were carried out at different angles φ, but all indicate rather mediocre Co–C bonding. Any reasonable geometry for the frame **31** was

(21) Burdett, J. K.; Albright, T. A. *Inorg. Chem.* **1979**, *18*, 2112 and references therein.

(22) Hoffmann, R. *Angew. Chem.* **1982**, *94*, 725.

(23) (a) Schaad, L. J.; Burnelle, L. A.; Dressler, K. P. *Theoret. Chim. Acta* **1969**, *15*, 91. (b) Andrē, J.-M.; Andrē, M.-C.; Leroy, G. *Chem. Phys. Lett.* **1969**, *3*, 695. (c) Buenker, R. J. *J. Chem. Phys.* **1968**, *48*, 1368.

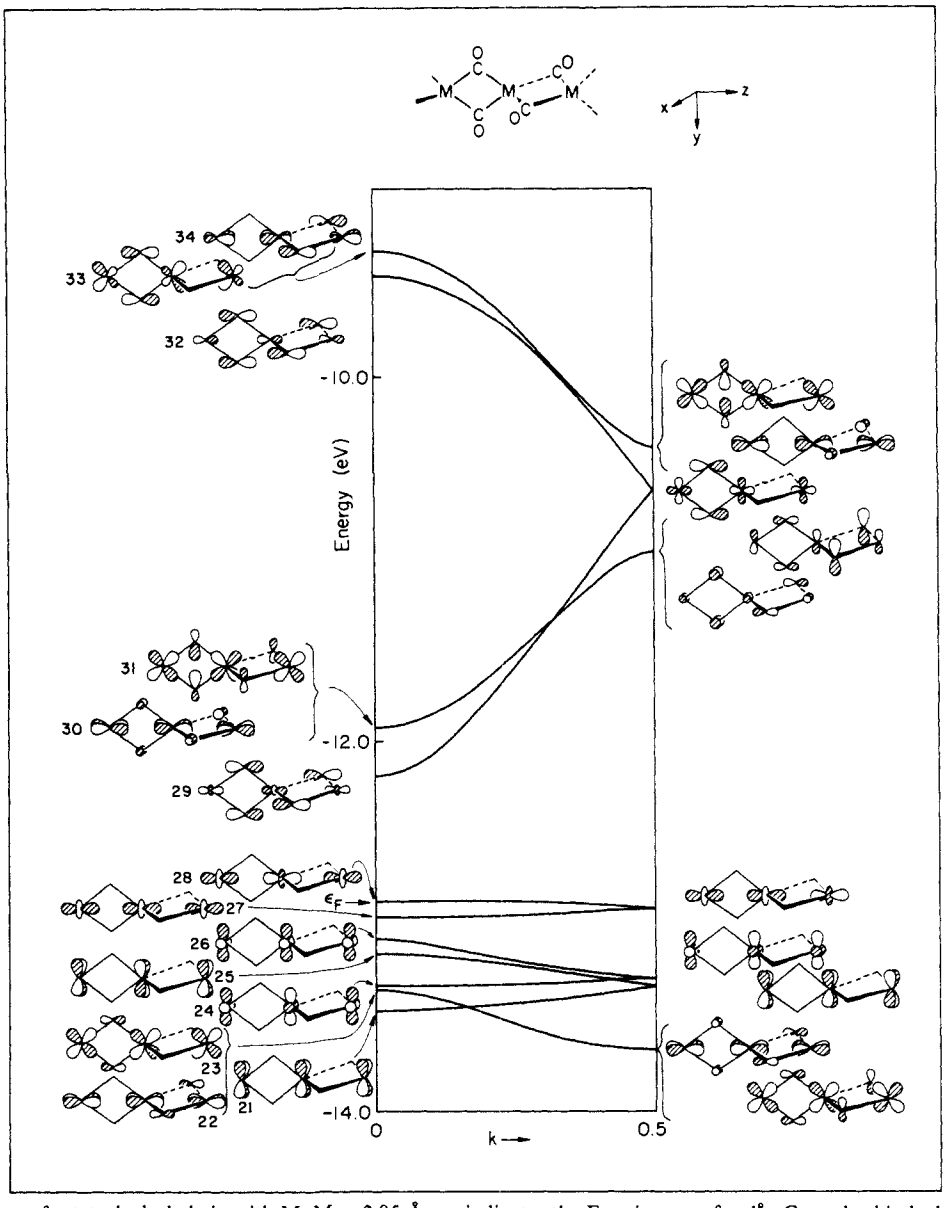

Figure 5. Band structure of a tetrahedral chain with M–M = 2.85 Å. ϵ_F indicates the Fermi energy for d^8. Crystal orbitals degenerate at the zone edge are pictured only once.

consistently computed to lie ~1.0 eV above the coplanar isomer.

Our concluding topic is short discussion concerning the hypothetical extended structures described earlier. As in the molecular case, we are interested in the dependence of geometry on electron count. In Figure 4 we present results of some exploratory calculations on five one-dimensional chains, **a**–**e**, for electron counts corresponding to d^6 through d^{10} at the metal. The intercell metal–metal distances were fixed at 2.36 Å, as in the observed molecular structure, and cobalt atomic parameters were used throughout. For each metal, the zero of energy is defined by the lowest energy structure.

By analogy to molecular chemistry, we would predict a preference for square-planar geometries at high d-electron counts. This is indeed the case; the two lowest energy Ni-d^{10} structures, **b** and **d**, are square planar about the metal centers. Toward the left in the transition-metal series, we expect a propensity for high coordination and increased metal–metal bonding. This trend is well illustrated by the monotonic increase in the stability of the double chain **a** as the electron count is lowered. The local environment of the bridging metal dimers in **a** is very suggestive of the M_2L_8 geometry so common for chromium.[24] This high-coordinate structure is one of the lowest energy configurations for Cr-d^6; the energy difference is too small to specify the exact ordering.

The planar **b** and tetrahedral **e** chains are of particular interest in light of our molecular calculations. At this metal–metal distance, it is only for nickel that the planar chain is favored over the tetrahedral. A similar picture emerges as the metal–metal bond is lengthened to 2.85 Å; now, however, both nickel and cobalt prefer the planar geometry. We will not dwell on the effects of bond lengthening and shortening in one-dimensional chains, as this has recently been thoroughly discussed by two of us.[25]

It is curious to see that contrary to the molecular case, cobalt prefers the puckered chain **d** over both the planar **b** and tetrahedral **e**, although the energy increase for the latter is small. We are still puzzled by this result.

We will present only one band structure, that of the tetrahedral chain. It is particularly interesting in that for iron it is not only the most stable configuration at Fe–Fe = 2.36 Å but it also has a gap at the Fermi level which widens as the intermetallic separation increases. We have chosen M–M = 2.85 Å to produce the band structure shown in Figure 5. The character of the bands changes little from the elongation and only the dispersion is reduced.

(24) Cotton, F. A.; Walton, R. A. "Multiple Bonds Between Metal Atoms"; Wiley-Interscience: New York, 1982.

(25) Silvestre, J.; Hoffmann, R. *Inorg. Chem.* **1985**, *24*, 4108.

Table II. Extended Hückel Parameters

orbital		H_{ii}, eV	exponents[a] ζ_1	ζ_2
H	1s	-13.4	1.3	
C	2s	-21.4	1.62k	
	2p	-11.4	1.625	
O	2s	-32.3	2.275	
	2p	-14.8	2.275	
Co	4s	-9.21	2.0	
	4p	-5.29	2.0	
	3d	-13.18	5.55 (0.5679)	2.10 (0.6059)

[a] Two Slater exponents are listed for 3d functions. Each is followed in parentheses by the coefficients in the double-ζ expansion.

Can we rationalize this band structure in terms of the familiar two below three splitting of tetrahedral molecular complexes reproduced in **32**? Since there are two metal atoms per unit cell,

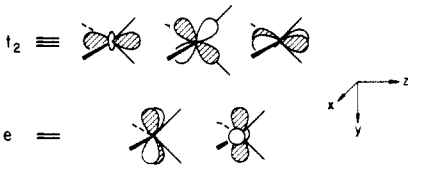

32

we should find two bands of each type in Figure 5. The e set clearly transforms into the clustered bands 21, 24, 25, and 26. They lie below the Fermi energy for d^8 and are quite narrow as the interaction is of δ type. Because the intermetallic distance is large, we expect to locate the six t_2 set bands directly above these four, but only the z^2 bands 27 and 28 appear where predicted. The intracell antibonding xz and yz combinations form the degenerate bands 22 and 23. They are pushed down by a σ-bonding interaction with the carbonyl π^*, as shown in **33**, for example, at the zone center for yz. The intracell bonding counterparts become the degenerate pair 30 and 31. Their interaction with the carbonyl π^* is π bonding, but the effect is over shadowed by their σ antibonding character with the carbonyl lone pairs, as sketched in **34** for yz at the zone center. The bands are pushed high up in energy and undergo an avoided crossing with the degenerate set 33 and 34 which carry the d character at the zone edge. The net result is a four below one splitting which although

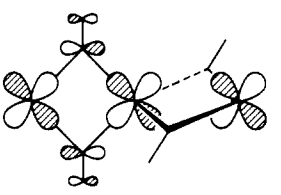

33

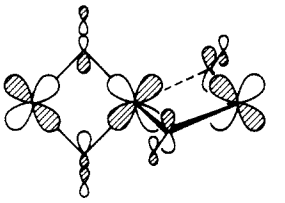

34

unusual for tetrahedral coordination is certainly comfortable for the d^8 system.

It seems reasonable that somewhere one or more of these polymeric structures has already been created but has been lost in the tar of a reaction vessel. Their existence would not be without precedence. Take, for instance, the alkoxy polymers[26] or Haines' polymeric $[Rh_2(\mu_2\text{-}Cl)_2(\mu_2\text{-}PH_2)_2(CO)_2]_n$[27] which assumes the geometry of **c** with pendant CO groups. Given the variety and abundance of structures utilizing the carbonyl ligand in molecular organometallic chemistry, we think it is not unlikely that in due time the carbonyl unit will prove to be just as versatile and productive in the field of solid-state chemistry. We await the synthetic and structural work that will move us from speculations to real chemistry.

Acknowledgment. We are grateful to the National Science Foundation for its support of this work through Research Grant CHE 8406119. Thanks are extended to Jane Jorgensen and Elisabeth Fields for careful rendering of the drawings.

Appendix

The calculations were of the extended Hückel type with weighted H_{ij}'s[29] with parameters (see Table II) taken from previous work.[30] Distances used throughout are Co–Co = 2.36 Å, Co–C = 1.82 Å, C–O = 1.20 Å, Co–Cp centroid = 1.724 Å. The geometry of molecular and extended "puckered" structures was defined by setting C–C = 2.36 Å for carbonyls straddling the metal–metal bond.

(26) Bradley, D. C.; Mehrotra, R. C.; Gaur, D. P. "Metal Alkoxides"; Academic Press: New York, 1978.
(27) Haines, R. J.; Sleen, N. D. C. T.; English, R. B. *J. Chem. Soc., Dalton Trans.* **1983**, 1607.
(28) Hoffmann, R. *J. Chem. Phys.* **1963**, *39*, 1397.
(29) Ammeter, J. H.; Bürgi, H.-B.; Thibeault, J. C.; Hoffmann, R. *J. Am. Chem. Soc.* **1978**, *100*, 3686.
(30) Hoffman, D. M.; Hoffmann, R.; Fisel, C. R. *J. Am. Chem. Soc.* **1982**, *104*, 3858.

Reaction of Phenylchlorocarbene in Oxygen-Doped Matrices

George A. Ganzer,[†] Robert S. Sheridan,*[†] and Michael T. H. Liu[‡]

Contribution from the S. M. McElvain Laboratories of Organic Chemistry, Department of Chemistry, University of Wisconsin, Madison, Wisconsin 53706, and the Department of Chemistry, University of Prince Edward Island, Charlottetown, Prince Edward Island, Canada C1A AP3. *Received July 11, 1985*

Abstract: Irradiation of phenylchlorodiazirine at 10 K matrix isolated in argon gives phenylchlorocarbene. The carbene was characterized by IR, UV, and trapping with HCl. Warming an argon matrix containing O_2 and the carbene to 35 K caused reaction to give the corresponding carbonyl oxide. The yellow-green (λ_{max} 400 nm) carbonyl oxide was characterized by IR, UV, and $^{18}O_2$ labeling. Photolysis of the carbonyl oxide with visible light gave the corresponding dioxirane, benzoyl chloride, and ozone. The dioxirane, which showed only absorption tailing into the visible, was characterized by IR, $^{18}O_2$ labeling, and subsequent photochemistry. Irradiation of the dioxirane ($\lambda > 420$ nm) gave mainly phenyl chloroformate and a small amount of chlorobenzene and CO_2. Possible mechanisms for the novel spin-forbidden O_2 addition are discussed.

Carbonyl oxides and the isomeric dioxiranes have generated considerable interest as intermediates in ozonolyses,[1] and in oxidations of diazo compounds,[2] carbenes,[3] and carbonyl compounds.[4] Recently, several groups have reported direct observations of

[†] University of Wisconsin.
[‡] University of Prince Edward Island.

(1) Bailey, P. S. "Ozonation in Organic Chemistry"; Academic Press: New York, 1978; Vol. 1.

0002-7863/86/1508-1517$01.50/0